

# Diagnostic value of multi-slice spiral computed tomography combined with carcinoembryonic antigen and Wnt pathway inhibitor for early-stage lung cancer

X. Zhang<sup>1#</sup>, X. Wu<sup>2#</sup>, G. Wang<sup>3\*</sup>

<sup>1</sup>Department of Respiratory and Critical Care Medicine, The official name of our hospital has been changed into 301 Hospital, Beijing, China

<sup>2</sup>Department of Respiratory and Critical Care Medicine, Jiangxi Provincial People's Hospital (The First Affiliated Hospital of Nanchang University), Nanchang, Jiangxi Province, China

<sup>3</sup>Department of Radiology, Zhejiang Lishui People's Hospital, Lishui, Zhejiang Province, China

## ► Original article

## ABSTRACT

### \*Corresponding author:

Gaobo Wang, M.D.,

### E-mail:

becky.shaw133049@yahoo.com

Received: October 2024

Final revised: May 2025

Accepted: June 2025

Int. J. Radiat. Res., January 2026;  
24(1): 103-108

DOI: 10.61186/ijrr.24.1.16

**Keywords:** Carcinoembryonic antigen, diagnosis, lung neoplasms, CT.

#These authors contributed equally to this study.

**Background:** We aimed to analyze the significance of multi-slice spiral computed tomography (CT) combined with carcinoembryonic antigen (CEA) and Wnt pathway inhibitor (DKK1) for the diagnosis of early-stage lung carcinoma. **Materials and Methods:** Subjects (102 in total) were selected from patients with suspected early-stage lung carcinoma receiving treatment in the hospital. Multi-slice spiral CT was performed on all subjects, CEA and DKK1 levels in the serum were detected, and the diagnostic efficiency of multi-slice spiral CT for early-stage lung cancer was analyzed. **Results:** The sensitivity of 94.25% (82/87), Youden index of 0.743, specificity of 80.00% (12/15), accuracy of 92.16% (94/102), positive diagnostic value of 96.47% (82/85), and negative diagnostic value of 70.59% (12/17) were obtained for multi-slice spiral CT in diagnosing early-stage lung cancer. As revealed by receiver operating characteristic curve analysis results, multi-slice spiral CT parameters combined with CEA and DKK1 had an area under the curve of 0.954, sensitivity of 95.22% and specificity of 86.17% in the diagnosis of early-stage lung carcinoma, significantly superior to multi-slice spiral CT parameters, CEA or DKK1 alone ( $P < 0.05$ ). **Conclusion:** The combination of CEA and DKK1 with multi-slice spiral CT can improve the diagnostic efficiency for early-stage lung cancer.

## INTRODUCTION

Lung cancer stems from the bronchial epithelium and gland due to many factors such as occupation, environment, diet and smoking, and it has become one of the main malignancies causing human death<sup>(1)</sup>. Since lung cancer has no obvious specific symptoms in the early stage, patients have often been in the mid-late stage when diagnosed, thus reducing the 5-year survival rate<sup>(2)</sup>. At present, many diagnosis methods are available for early-stage lung cancer, such as pathology, X-ray, and multi-slice spiral computed tomography (CT). Among them, pathology is often used as the gold standard for diagnosing lung cancer, but it is invasive and thus cannot be used as a routine auxiliary diagnostic method. X-ray examination consumes short time and low cost, but overlapping of lesions and tissues occurs easily, thus the overall accuracy is not high<sup>(3)</sup>. As a non-invasive imaging means characterized by high resolution, clear images, high scanning speed and quantitative detection, multi-slice spiral CT has been gradually used in the clinical diagnosis of early malignancies<sup>(4)</sup>. Low-dose multi-slice spiral CT has

been proven to reduce lung cancer mortality by 20%<sup>(5)</sup>. However, when used alone, it has the limitation of a high false positive rate (causing unnecessary psychological burden and repeated radiation exposure)<sup>(6)</sup>, so it urgently needs to be combined with serum markers to improve the specificity<sup>(7)</sup>.

The detection of serum tumor factors has many advantages such as minimal invasion and simple operation, so this method has been used to improve the diagnostic accuracy for early-stage lung cancer<sup>(8)</sup>. Carcinoembryonic antigen (CEA), as an acidic glycoprotein, is mainly expressed during embryonic development but hardly expressed in healthy adults. An increased CEA expression often indicates cell carcinogenesis, which has been proven to be related to the occurrence of lung cancer<sup>(9)</sup>. Combining CEA detection with CT scan can improve lung cancer diagnosis<sup>(10)</sup>. DKK1, a Wnt pathway inhibitor, is a secretory glycoprotein considered a participant in cell differentiation, proliferation and carcinogenesis, as well as a potent antagonist of the Wnt signaling pathway, which is highly expressed in serum, cells and tissues of lung cancer<sup>(11)</sup>. Existing evidence has verified that multi-slice spiral CT combined with

multiple markers can significantly improve the accuracy of TNM staging and has important guiding value for the early diagnosis of stage I lung cancer<sup>(12)</sup>. Similar combination modes have been successfully applied to the diagnosis of tumors such as gastric cancer<sup>(13)</sup> and colon cancer<sup>(14)</sup>, verifying the feasibility of cross-cancer application.

Although previous studies have explored combining serum markers and imaging for early lung cancer diagnosis, the novelty of this study lies in specifically evaluating the combined diagnostic value of multi-slice spiral CT with serum CEA and DKK1 for early-stage lung cancer, aiming to enhance the diagnostic specificity, reduce the false positive rate, and ultimately improve the prognosis.

## MATERIALS AND METHODS

### Subjects

The study was approved by the ethics committee of Zhejiang Lishui People's Hospital (approval No. ZLPH20200154) on January 5th, 2020. Written informed consent was signed by all patients. Subjects consisted of 102 patients suspected of early-stage lung cancer [61 males plus 41 females, age: 45-78 years old and (61.98±4.35) years old on average], who received treatment in the hospital between January 2020 and January 2023. Fifty-eight patients (56.9 %) were current or former smokers (median 30 pack-years, IQR 15-45). Eastern Cooperative Oncology Group performance status was 0-1 in 97 patients (95.1 %). Common comorbidities included hypertension (34.3 %), diabetes mellitus (18.6 %), and chronic obstructive pulmonary disease (21.6 %). According to the 8th edition TNM classification, 78 tumors (76.5 %) were stage IA and 24 (23.5 %) were stage IB.

Inclusion criteria covered: 1) Patients suspected of early-stage lung cancer, with symptoms such as hoarseness, chest tenderness, dry cough, expectoration, and fever, 2) those who had undergone imaging examination and detection of serum CEA and DKK1, and had complete clinical and imaging data, 3) those pathologically diagnosed, and 4) those without dysfunction of liver, kidney and other vital organs. Exclusion criteria involved: 1) Patients with metastatic lung cancer, 2) those with a history of radiotherapy or chemotherapy for malignant tumors, 3) those with a history of lung surgery, 4) those with tumors at other sites, 5) those allergic to iodine, or 6) those who could not cooperate due to mental disorders, consciousness disorders or communication disorders.

### Multi-slice spiral CT

A 64-row 128-slice volume CT scanner (GE, USA) was used. During the examination, the patients were instructed to hold their breath, and scanned from the

sternoclavicular joint as the baseline to the base of lung through an appropriate lung window. The following scanning parameters were adopted: tube current =320 mA, matrix =512×512, pitch 0.9, slice thickness + gap =5.0 mm, collimation =64×0.625 mm, and tube voltage =100 kV. When the lung nodules were found, the reconstructed slice thickness was changed to 0.625 mm, prior to injection of 70 mL of nonionic iohexol (a contrast medium) at 3.0 mL/s as well as scanning within 30 s. Then the scanning images were transmitted to the workstation and read by two experienced radiologists independently and blindly (without knowing the pathological examination results). The scanning results were analyzed by the principle of consistency. In detail, when the results were consistent, they were directly given. If the results were inconsistent, a discussion was held, or a third experienced radiologist was consulted until a consensus was reached. CT signs (nodule-lung interface, classification and size of nodules, spicule sign, lobulation sign and pleural indentation) and CT scanning parameters [permeability surface (PS), mean transit time (MTT), blood flow (BF), peak enhancement intensity (PEI), and blood volume (BV)] were analyzed.

### Detection of serum CEA and DKK1

Venous blood (3 mL) collected from each fasted patient was centrifuged at 3500 rpm to isolate the serum. Then the levels of serum CEA and DKK1 were measured by electrochemiluminescence assay and its matching reagents (Roche Diagnostics GmbH, Germany), and by enzyme-linked immunosorbent assay using an automatic microplate reader and its matching reagents (Thermo Fisher Scientific, USA), respectively.

### Diagnostic indicators

All patients underwent CT-guided lung puncture biopsy, and the obtained lung nodule tissues were subjected to pathological examination. With the results of pathological examination as the gold standard, the diagnostic value of multi-slice spiral CT for early-stage lung cancer was determined. The following formula was employed to calculate the diagnostic efficiency: accuracy (%) = (true positive cases + true negative cases)/total cases×100%, sensitivity (%) = true positive cases/(true positive cases + false negative cases)×100%, specificity (%) = true negative cases/(false positive cases + true negative cases)×100%, Youden index = sensitivity + specificity-1, negative diagnostic value (%) = true negative cases/(false negative cases + true negative cases)×100%, and positive diagnostic value (%) = true positive cases/(true positive cases + true negative cases)×100%.

### Statistical analysis

Analysis and processing were accomplished by

SPSS 25.0 software (IBM Inc., USA). The expression format of mean  $\pm$  standard deviation ( $\bar{x} \pm s$ ) together with independent-samples *t*-test for comparison between two groups was adopted for measurement data. Frequency and percentage were utilized to describe enumeration data, which were compared between two groups by the  $\chi^2$  test. Receiver operating characteristic (ROC) curves were constructed to probe into the diagnostic value of multi-slice spiral CT parameters, CEA and DKK1 for early-stage lung cancer.  $P < 0.05$  was considered statistically significant.

## RESULTS

### Diagnostic efficiency of multi-slice spiral CT for early-stage lung cancer

With pathology as the gold standard, 87 out of 102 suspected cases of early-stage lung cancer were pathologically diagnosed with early-stage lung cancer, and the remaining 15 cases were diagnosed with benign lung diseases (figure 1). Furthermore, the sensitivity of 94.25% (82/87), Youden index of 0.743, specificity of 80.00% (12/15), accuracy of 92.16% (94/102), positive diagnostic value of 96.47% (82/85), and negative diagnostic value of 70.59% (12/17) were obtained for multi-slice spiral CT in diagnosing early-stage lung cancer (table 1).



**Figure 1.** A sample image of multislice CT for lung cancer with a red arrow indicating the region of interest. CT: Computed tomography.

**Table 1.** Diagnostic efficiency of multi-slice spiral CT for early-stage lung cancer.

Method	Result	Gold standard (pathology)		Total
		Positive	Negative	
Multi-slice spiral CT	Positive	82	3	85
	Negative	5	12	17
Total		87	15	102

CT: Computed tomography.

### Multi-slice spiral CT signs of early-stage lung carcinoma and benign pulmonary diseases

The proportion of blurred nodule-lung interface, part-solid nodules, nodule size  $\geq 3$  cm, spicule sign, lobulation sign and pleural indentation was increased in subjects with early-stage lung carcinoma by contrast with that in subjects suffering from benign lung diseases ( $P < 0.05$ ) (table 2).

### Multi-slice spiral CT parameters early-stage lung carcinoma and benign pulmonary diseases

In comparison to patients affected by benign lung

diseases, those suffering early-stage lung carcinoma had increased MTT, BV and PS, but decreased PEI and BF ( $P < 0.05$ ) (table 3).

**Table 2.** Multi-slice spiral CT signs of patients suffering early-stage lung carcinoma and benign pulmonary diseases [n (%)].

Multi-slice spiral CT signs	Early-stage lung cancer (n=87)	Benign lung diseases (n=15)	$\chi^2$	P	
Nodule-lung interface	Clear	5 (5.75)	11 (73.33)	47.040	<0.001
	Less clear	14 (16.09)	3 (20.00)		
	Blurred	68 (78.16)	1 (6.67)		
Classification of nodules	Pure ground-glass	25 (28.74)	7 (46.67)	9.610	0.008
	Part-solid	48 (55.17)	2 (13.33)		
	Solid	14 (16.09)	6 (40.00)		
Size of nodules (cm)	$\geq 3$	67 (77.01)	2 (13.33)	23.704	<0.001
	<3	20 (22.99)	13 (86.67)		
Spicule sign	Yes	75 (86.21)	3 (20.00)	31.168	<0.001
	No	12 (13.79)	12 (80.00)		
Lobulation sign	Yes	69 (79.31)	1 (6.67)	31.359	<0.001
	No	18 (20.69)	14 (93.33)		
Pleural indentation	Yes	67 (77.01)	2 (13.33)	23.704	<0.001
	No	20 (22.99)	13 (86.67)		

CT: Computed tomography.

**Table 3.** Multi-slice spiral CT parameters of subjects suffering early-stage lung carcinoma and benign pulmonary diseases ( $\bar{x} \pm s$ ).

Multi-slice spiral CT parameter	Early-stage lung cancer (n=87)	Benign lung diseases (n=15)	<i>t</i>	P
MTT (s)	9.12 $\pm$ 1.29	8.00 $\pm$ 1.09	3.170	0.002
PEI (Hu)	28.97 $\pm$ 2.45	33.24 $\pm$ 3.23	5.935	<0.001
BF (ml/min·100g)	67.84 $\pm$ 8.79	85.64 $\pm$ 9.83	7.119	<0.001
BV (ml/100g)	4.14 $\pm$ 0.26	3.57 $\pm$ 0.25	7.883	<0.001
PS (ml/min·100g)	16.57 $\pm$ 2.23	11.23 $\pm$ 1.96	8.705	<0.001

CT: Computed tomography; BF: blood flow; BV: blood volume; MTT: mean transit time; PEI: peak enhancement intensity; PS: permeability surface.

### Levels of serum CEA and DKK1 in participants with early-stage lung carcinoma and benign pulmonary diseases

CEA and DKK1 exhibited raised levels in the serum of patients with early-stage lung cancer compared with those of subjects affected by benign lung diseases ( $P < 0.05$ ) (table 4).

**Table 4.** CEA and DKK1 levels in the serum of participants with early-stage lung cancer and benign lung diseases [ $(\bar{x} \pm s)$ , ng/mL].

Indicator	Early-stage lung cancer (n=87)	Benign lung diseases (n=15)	$\chi^2$	P
CEA	5.67 $\pm$ 0.98	2.11 $\pm$ 0.13	13.990	<0.001
DKK1	37.57 $\pm$ 4.35	11.23 $\pm$ 1.98	22.970	<0.001

CEA: Carcinoembryonic antigen; DKK1: Wnt pathway inhibitor.

### Diagnostic efficiency of multi-slice spiral CT parameters and CEA and DKK1 for early-stage lung cancer

According to ROC curve analysis, the combination of multi-slice spiral CT parameters presented the area under the curve (AUC), sensitivity and specificity of 0.923, 90.23% and 88.63%, respectively, for diagnosing early-stage lung carcinoma, which were significantly higher than those of any multi-slice

spiral CT parameter alone ( $P < 0.05$ ) (figure 2). Moreover, multi-slice spiral CT parameters combined with CEA and DKK1 had an AUC of 0.954, sensitivity of 95.22% and specificity of 86.17% in the diagnosis of early-stage lung cancer, which were significantly higher than those of multi-slice spiral CT parameters, CEA or DKK1 alone ( $P < 0.05$ ) (figure 3).

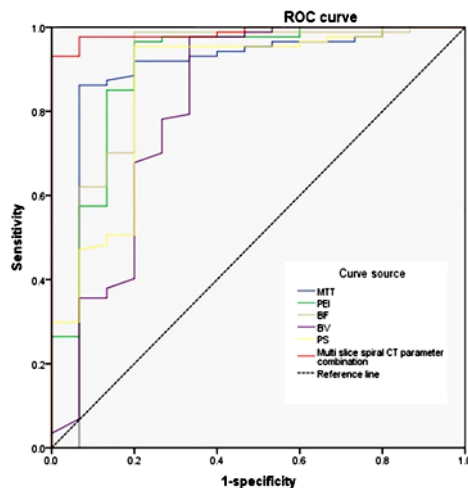


**Figure 2.** ROC curve of multi-slice spiral CT parameters for diagnosing early-stage lung carcinoma. CT: Computed tomography; ROC: receiver operating characteristic.

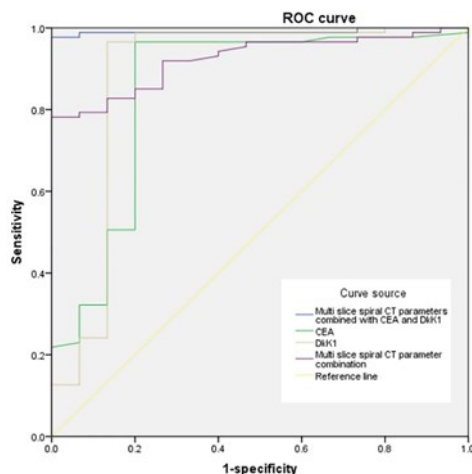


**Figure 3.** ROC curve for CEA and DKK1 in combination with multi-slice spiral CT parameters in the diagnosis of early-stage lung cancer. CEA: Carcinoembryonic antigen; CT: computed tomography; DKK1: Wnt pathway inhibitor; ROC: receiver operating characteristic.

## DISCUSSION

Multi-slice spiral CT can scan the same part and the whole organ volume, achieving all-around detection of lesions and avoiding omissions. Meanwhile, lesion and tissue artifacts can also be eliminated to improve image quality (15). The actual condition of pulmonary perfusion can be clearly understood using contrast media when diagnosing early-stage lung carcinoma by multi-slice spiral CT, thereby observing vascular endothelial cells (16,17). In this study, multi-slice spiral CT effectively

distinguished early-stage lung cancer from benign lung diseases. Compared to the gold standard of pathology, multi-slice spiral CT presented the accuracy and specificity of 94.25% and 80.00%, respectively. Similarly, Xiang *et al.* (18) confirmed that multi-slice spiral CT effectively distinguished localized lung adenocarcinoma from localized lung inflammation. Furthermore, patients with early-stage lung cancer mainly exhibited part-solid nodules with unclear boundaries, and they mostly showed spicule signs, suggesting that early-stage lung cancer had typical imaging features.

CEA is a marker commonly used in the diagnosis of malignancies, and its elevated level is an important contributor to the progression of malignancies (19). Only a small amount or no expression of CEA is detected in the peripheral blood of healthy people, but its expression increases after tissue cancerization (20, 21). Possibly, after the change in tumor blood supply and tumor necrosis, CEA is released as dissolved fragments into the peripheral circulation, thus increasing the CEA level. Zhou *et al.* (22) found that after being released into the blood, CEA caused an escape of cancer cells from immune surveillance, interfered with intercellular adhesion, and constantly invaded surrounding tissues and even distant tissues. Besides, Li *et al.* (23) reported that the expression of CEA was elevated with increasing malignancy degree of lung cancer. Consistently, we herein also found that the serum CEA displayed a high expression in subjects with early-stage lung cancer.

DKK1 is the first discovered secretory inhibitor of the Wnt pathway (24, 25). It can form endosomes synergistically with Kremen protein by conjugating with low-density lipoprotein receptor-related protein 5/6, so as to inhibit Wnt signaling, which is implicated in the occurrence and prognosis of rheumatoid arthritis and osteoarthritis. Moreover, DKK1 can cooperate with the tumor inhibitor p53 to antagonize the abnormal Wnt pathway activation, affecting cancerous cell proliferation and invasion (26). It is an important player in intrinsic, innate and adaptive anti-tumor immunoregulation, and can affect tumor immune microenvironment and participate in the occurrence of malignancies, as a diagnostic marker for malignancies (27). At present, the increased expression of DKK1 in various malignancies covering ovarian cancer, breast cancer and colorectal cancer has been verified (28). In this study, patients suffering early-stage lung cancer had evidently raised expression of serum DKK1 compared to those with benign lung diseases, being consistent with the results reported by Sun *et al.* (29) Taken together, CEA and DKK1 may be involved in the occurrence of early-stage lung cancer.

ROC curves were employed to investigate the diagnostic efficiency of multi-slice spiral CT in combination with CEA and DKK1 for early-stage lung cancer in the present study. For the diagnosis of early

-stage lung carcinoma, the sensitivity and specificity of the combination of multi-slice spiral CT parameters were 90.23% and 88.63%, respectively, which were significantly higher than those of any multi-slice spiral CT parameter alone. Furthermore, multi-slice spiral CT parameters combined with CEA and DKK1 had the sensitivity of 95.22% and specificity of 86.17% for diagnosing early-stage lung cancer, suggesting a significantly augmented diagnostic efficiency. Collectively, multi-slice spiral CT combined with serum tumor factors had a higher diagnostic accuracy for early-stage lung cancer.

Nevertheless, this study is limited. First, the sample size is small. Second, only two serum tumor factors are tested. In the future, more cases and serum tumor factors will be studied to confirm our findings.

## CONCLUSION

In conclusion, multi-slice spiral CT combined with CEA plus DKK1 is capable of enhancing the diagnostic efficiency of early-stage lung carcinoma.

**Acknowledgment:** None.

**Funding:** None.

**Conflicts of interest:** The authors of this article affirm that they have none about this topic.

**Ethical consideration:** The study was approved by the ethics committee of Zhejiang Lishui People's Hospital (approval No. ZLPH20200154) on January 5th, 2020.

**Author contribution:** X.Z. designed this study and significantly revised the manuscript; X.W. and G.W. performed this study and writing manuscript.

## REFERENCES

- Sun YJ, Lou J, Xu QL, et al. (2021) Comparison of clinical diagnostic value of spiral CT with different dose in patients with early-stage peripheral lung cancer. *Clin Transl Oncol*, **23(6)**: 1128-1133. doi: 10.1007/s12094-020-02503-7
- Lee E and Kazerooni EA (2022) Lung Cancer Screening. *Semin Respir Crit Care Med*, **43(6)**: 839-850. doi: 10.1055/s-0042-1757885
- Foley RW, Nassour V, Oliver HC, et al. (2021) Chest X-ray in suspected lung cancer is harmful. *Eur Radiol*, **31(8)**: 6269-6274. doi: 10.1007/s00330-021-07708-0
- Liu H, Wang H, Xiong C, et al. (2023) Efficacy of Multi-slice Spiral CT and rapid on-site evaluation in diagnosis of pulmonary nodules. *Altern Ther Health Med*, **17**: AT9079.
- Gasparri R, Sabalic A, Spaggiari L (2023). The early diagnosis of lung cancer: Critical gaps in the discovery of biomarkers. *J Clin Med*, **12(23)**: 7244. doi: 10.3390/jcm12237244
- Zhang Y, Liu W, Zhang H, et al. (2023). Extracellular vesicle long RNA markers of early-stage lung adenocarcinoma. *Int J Cancer*, **152(7)**: 1490-1500. doi: 10.1002/ijc.34386
- Wang L, Tian G, Zhang H, et al. (2024). Prognostic value of CT perfusion imaging, serum DD and MMP-9 on hemorrhage transformation after thrombolysis in patients with acute cerebral infarction. *Int J Radiat Res*, **22(3)**: 711-717. doi: 10.61186/ijrr.22.3.711
- Thai AA, Solomon BJ, Sequist LV, et al. (2021) Lung cancer. *Lancet*, **398(10299)**: 535-554. doi: 10.1016/S0140-6736(21)00312-3
- Cheng C, Yang Y, Yang W, et al. (2022) The diagnostic value of CEA for lung cancer-related malignant pleural effusion in China: a meta-analysis. *Expert Rev Respir Med*, **16(1)**: 99-108. doi: 10.1080/17476348.2021.1941885
- Liu M, Zhou Z, Liu F, et al. (2022) CT and CEA-based machine learning model for predicting malignant pulmonary nodules. *Cancer Sci*, **113(12)**: 4363-4373. PubMed: 36056603, DOI: https://doi.org/10.1111/cas.15561
- Ren W, Li Y, Chen X, et al. (2022) RYR2 mutation in non-small cell lung cancer prolongs survival via down-regulation of DKK1 and up-regulation of GS1-115G20.1: A weighted gene Co-expression network analysis and risk prognostic models. *IET Syst Biol*, **16(2)**: 43-58. doi: 10.1049/syb2.12038
- Zhang Y, Sun B, Yu Y, et al. (2024) Multimodal fusion of liquid biopsy and CT enhances differential diagnosis of early-stage lung adenocarcinoma. *NPJ Precis Oncol*, **8(1)**: 50. doi: 10.1038/s41698-024-00551-8
- Zhao GN, Du XS, Zhou PZ, et al. (2023). Comparison of clinical value and diagnostic rate between barium meal radiography and spectral CT scan in the diagnosis and treatment of gastric cancer and benign gastric tumor. *Int J Radiat Res*, **21(4)**: 639-645. doi: 10.61186/ijrr.21.4.639
- Yang H and Chu Y (2025) Clinical value of multi-slice spiral CT in evaluating preoperative TNN staging and postoperative recurrence and metastasis of colon carcinoma. *SLAS Technol*, **31**: 100247. doi: 10.1016/j.slast.2025.100247
- Zhao S, Bi Y, Wang Z, et al. (2022) Accuracy evaluation of combining gastroscopy, multi-slice spiral CT, Her-2, and tumor markers in gastric cancer staging diagnosis. *World J Surg Oncol*, **20(1)**: 152. doi: 10.1186/s12957-022-02616-z
- Xiang Y, Zhang M, Zhao W, et al. (2023) Differentiation of localized pneumonic-type lung adenocarcinoma from localized pulmonary inflammatory lesion based on clinical data and multi-slice spiral computed tomography imaging features. *Transl Cancer Res*, **12(1)**: 113-124. doi: 10.21037/tcr-22-2525
- Wang S, Xu F, Wang Y, et al. (2023) Relevant risk factor and follow-up of lung nodules in physical examination with low-dose ct screening. *Iran J Public Health*, **52(2)**: 350-359. doi: 10.18502/ijph.v52i2.11888
- Xiang Y, Zhang M, Zhao W, et al. (2023) Differentiation of localized pneumonic-type lung adenocarcinoma from localized pulmonary inflammatory lesion based on clinical data and multi-slice spiral computed tomography imaging features. *Transl Cancer Res*, **12(1)**: 113-124. doi: 10.21037/tcr-22-2525
- Tian K, Li Z, Qin L (2022) Detection of CEA and ProGRP Levels in BALF of Patients with Peripheral Lung Cancer and Their Relationship with CT Signs. *Biomed Res Int*, **2022**: 4119912. doi: 10.1155/2023/9810949
- Yajima S, Nakanishi Y, Matsumoto S, et al. (2022) Prognostic significance of the postoperative/preoperative serum CEA level ratio in patients with solitary adrenal metastasis from lung cancer. *Mol Clin Oncol*, **16(1)**: 10. doi: 10.3892/mco.2021.2443
- Li G, Zhang H, Zhang L, et al. (2022) Serum markers CA125, CA153, and CEA along with inflammatory cytokines in the early detection of lung cancer in high-risk populations. *Biomed Res Int*, **2022**: 1394042. doi: 10.1155/2024/9827549
- Zhou W, Yang Y, Wang Z, et al. (2021) Impact of HSP90 $\alpha$ , CEA, NSE, SCC, and CYFRA21-1 on lung cancer patients. *J Healthc Eng*, **2021**: 6929971. doi: 10.1155/2023/9796148
- International BR (2024) Retracted: Serum Markers CA125, CA153, and CEA along with inflammatory cytokines in the early detection of lung cancer in high-risk populations. *Biomed Res Int*, **2024**: 9827549. doi: 10.1155/2024/9827549
- Shi T, Zhang Y, Wang Y, et al. (2022) DKK1 promotes tumor immune evasion and impedes anti-PD-1 treatment by inducing immunosuppressive macrophages in gastric cancer. *Cancer Immunol Res*, **10(12)**: 1506-1524. doi: 10.1158/2326-6066.CIR-22-0218
- Gao S, Jin Y, Zhang H (2021) Pan-cancer analyses reveal oncogenic and immunological role of dickkopf-1 (DKK1). *Front Genet*, **12**: 757897. doi: 10.3389/fgene.2021.757897
- Ding G, Lu W, Zhang Q, et al. (2021) ZBTB38 suppresses prostate cancer cell proliferation and migration via directly promoting DKK1 expression. *Cell Death Dis*, **12(11)**: 998. doi: 10.1038/s41419-021-04278-3
- Huo Q, Xu C, Shao Y, et al. (2021) Free CA125 promotes ovarian cancer cell migration and tumor metastasis by binding Mesothelin to reduce DKK1 expression and activate the SGK3/FOXO3 pathway. *Int J Biol Sci*, **17(2)**: 574-588. doi: 10.7150/ijbs.52097

28. Liang T, Wu X, Wang L, *et al.* (2023) Correlation of NNMT and DKK1 protein expression with clinicopathological characteristics and prognosis of breast cancer. *Clin Med Insights Oncol*, **17**: 11795549231168073. doi. 10.1177/11795549231168073
29. Sun J, Chen X, Wang Y (2020) Comparison of the diagnostic value of CEA combined with OPN or DKK1 in non-small cell lung cancer. *Oncol Lett*, **20(3)**: 3046-3052. doi. 10.3892/ol.2020.11846